Available online at www.sciencedirect.com
SCIENCE DIRECT®
International Journal of Heat and Mass Transfer 48 (2005) 2548–2560
International Journal of HEAT and MASS TRANSFER
www.elsevier.com/locate/ijhmt

Entropy generation in conduits filled with porous medium totally and partially

T.V. Morosuk *

Refrigeration Machines Department, Odessa State Academy of Refrigeration, 1/3 Dvorianskaya St., Odessa 65026, Ukraine

Received 15 March 2004
Available online 31 March 2005

Abstract

Exergy or entropy generation analysis as a tool of applied thermodynamics is becoming standard practice for optimizing energy conversion systems and in identifying the deficiency of a component in a system. Porous media is used to enhance heat transfer in heat exchangers (HE). Also, porous layer adjusted to the inner surface simulates the fouling effect in heat exchangers. Optimizing the heat exchanger inserted with porous media and understanding the fouling effect on the rate of heat transfer and fluid flow is crucial for HE design and operations, which motivate the present work. The present work mainly investigates entropy generation due to flow in a pipe fully or partially filled with porous medium. The pipe is assumed to be isothermal. The porous layer is inserted at the core of the pipe or attached on the inner surface of the pipe. Forced, laminar flow is assumed. The effects of porous layer thickness and permeability of layer on the rate of entropy generation were investigated. Developing and fully developed flow conditions are considered in the analysis.

1. Introduction

Entropy generation in energy conversion systems is discussed by Bejan [1] and Bejan et al. [2]. Exergy analysis is important for system optimizations especially for heat exchangers (HE), where pumping power (pressure drop) and rate of heat transfer should be optimized for the best performance of the HE.

Hence, for optimization problems of HE by adapting exergy analysis it is necessary to determine the following parameters, value of exergy destruction (E_D), value of exergy losses (E_L), capital investment cost (Z^{CI}) and operational and maintenance cost ($Z^{O\&M}$) of HE.

Exergy destruction (E_D) mainly cased by temperature difference and pressure drop in the HE and exergy losses (E_L) is due to heat losses to the environment. The temperature difference determines capital investment cost and operational and maintenance cost as function $Z = Z^{CI} + Z^{O\&M} = f(h, A, \Delta T)$, which can be estimated based on heat transfer and fluid flow analysis. In the present study, it assumed that there is no heat transfer to the ambient; hence E_L is set to zero.

The exergy distraction can be related to entropy generation by using Guy–Stodola theorem as for jth component of energy conversion system:

$$E_{D,j} = T_{env} \cdot E_{g,j}. \quad (1)$$

Entropy minimization in heat exchangers considered by Bejan [1,3] and economical evaluation considered by De Olivera et al. [4]. The mentioned works considered

* Tel.: +380 482 239 183; fax: +380 482 238 931.
E-mail address: morosuk@paco.net

0017-9310/$ - see front matter © 2005 Elsevier Ltd. All rights reserved.
doi:10.1016/j.ijheatmasstransfer.2005.01.018

Nomenclature

Br_m	modified Brinkman number, $Br \cdot T_o/\Delta T$ [–]
c	specific heat [J/kg K]
D	pipe diameter [m]
Da	Darcy number, K/r_o^2 or $K/(H/2)^2$ [–]
e_g	specific entropy generation, [J/kg K]
E_g	dimensionless entropy generation, $(e_g r_o^2 T_o^2)/(k\nabla T^2)$ [–]
E_D	exergy destruction [J]
E_L	exergy losses [J]
F	inertia coefficient [–]
Gz	Graetz number, $4 \cdot Pr \cdot Re/Z$ [–]
H	half channel height [m]
h	heat transfer coefficient [W/m^2 K]
h_v	volumetric heat transfer coefficient [W/m^3 K]
k	thermal conductivity [W/m K]
K	permeability [m^2]
m	mass flow rate [kg/s]
Nu	Nusselt number [–]
p	pressure [Pa]
P	dimensionless pressure, $p/(\rho \cdot u_{in}^2)$ [–]
Pe	Peclet number, $Pr \cdot Re$ [–]
Pr	Prandtl number [–]
r	radial coordinate, radius [m]
R	dimensionless radius, r/r_o [–]
Re	Reynolds number, $\rho \cdot u_{in} \cdot r_o/\mu$ or $\rho \cdot u_{in} \cdot (H/2)/\mu$ [–]
Re_D	Reynolds number based on pipe diameter, $\rho \cdot u_{in} \cdot D/\mu$ [–]
Re_H	Reynolds number based on the channel height, $\rho \cdot u_{in\ H}/\mu$ [–]
R_p, Y_p	ratio of the porous medium radius to the pipe radius, or the porous layer thickness to the channel height, r_p/r_o,y_p/H [–]
T	temperature [K]
u	velocity component in z-direction [m/s]
U	dimensionless velocity in z-direction, u/u_{in} [–]
v	velocity component in r-direction [m/s]
V	dimensionless velocity in r-direction, v/u_{in} [–]
$\|u\|$	velocity magnitude, $(u^2 + v^2)^{0.5}$ [m/s]
$\|U\|$	dimensionless velocity magnitude, $(U^2 + V^2)^{0.5}$ [–]
y_p	half porous layer thickness [m]
z	axial coordinate [m]
Z	cost [EURO]
Z^{CI}	capital investment cost [EURO]
$Z^{O\&M}$	operational and maintenance cost [EURO]

Greek symbols

μ	viscosity [kg/m s]
θ	dimensionless temperature, $(T - T_{in})/(T_w - T_{in})$ [–]
ρ	density [kg/m^3]
ξ	dimensionless, z/r_o or z/H [–]

Subscripts

e	effective
env	environmental
f	fluid
in	inlet condition
m	bulk
o	outer radius of the tube
p	porous matrix radius/height
w	wall

simple heat exchanger without any heat transfer enhancement mechanisms. Also, the fouling problem in HE was considered by Robert and Feidt [5].

Partially filling a tube with porous media has two fold of applications; a layer of porous medium adjusted to the inner surface of a tube simulates the fouling, which is one of the main problems of the HE (Morosuk [6]). On the other hand, adding a porous cylinder to the core of the tube enhances heat transfer (Mohamad [7]). An over review will be given on the work done on application of porous layer for heat transfer enhancements.

Different methods of heat transfer enhancements in HE have been extensively studied and reviewed by Webb [8], then there is no need to elaborate on the topic. Using porous medium to enhance the rate of heat and mass transfer in HE has many advantages. The value of Nusselt number is few folds higher than the values predicted for laminar flows in channels without porous materials [7]. For high porous media, the enhancement of heat transfer is less than the value suggested by [9], which also depends on the effective thermal conductivity of the medium. Moreover, the radiative heat transfer is higher for systems filled with porous material than that without porous material due to the emitting and scattering properties of the porous solid surfaces. For some applications there is no need to completely fill the systems with the porous medium, as a partial filling of the porous medium is sufficient. Partial filling has advantage of reducing the pressure drop compared with a system filled completely with porous medium. Moreover, partial filling eliminates contact between the porous material and

surface, which decreases heat losses from the porous material to the surface. Such a criterion is required in a system where the main purpose is to enhance the thermal coupling between the porous medium and fluid flow, and to eliminate strong thermal coupling between the system and the ambient. For instance, in the solar air heater developed by Mohamad [10], the main idea was to enhance the rate of heat transfer from the porous medium, which is heated by solar radiation, to air, and at the same time to reduce the heat losses to the ambient. Furthermore, partial filling can reduce pressure drop. A partial filling of a channel with porous media forces the flow to escape from the core region, depending on the permeability of the medium, to the outer region, which reduces the boundary layer thickness and consequently enhances the rate of heat transfer. The porous medium also modifies the effective thermal conductivity and heat capacity of the flow, and the solid matrix enhances the rate of radiative heat transfer in a system where the gas is the working fluid. Hence, the heat transfer enhancements take place by three mechanisms; flow redistribution, thermal conductivity modification and radiative property modification of the medium.

Kaviany [11] considered laminar developing flow through a porous layer sandwiched between isothermal parallel plates. Forced convection in a channel whose walls are layered by a porous medium was considered by Poulikakos and Kazmierczak [12] for constant heat flux and constant wall temperature conditions, both analytically and numerically. A numerical study was presented by Jang and Chen [13] for a forced flow in a parallel channel partially filled with a porous medium by adopting the Darcy–Brinkman–Forchheimer model with a thermal dispersion term. Chikh et al. [14,15] presented an analytical solution for the fully developed flow in annulus configuration partially filled with porous medium. Al-Nimr and Alkam [16] extended the analysis to the transient solution for annulus flow with porous layer. Recently, Alkam et al. [17] and Abu-Hijleh and Al-Nimr [18] studied transient forced convection behavior of a flow in parallel plate channels with a porous substrate attached to the one of the plates. Recent reviews of the subject are available in [9,19].

In the present work, steady laminar flow in conduits (pipes and channels) partially filled with a porous layer was considered analytically and numerically for constant wall temperature boundary conditions. The entropy generations due to mechanical and thermal mechanisms are analyzed theoretically and numerically. The results are presented for different permeability and porous layer thicknesses. It is found that the mechanical entropy generation is most dominant mechanism of irreversibility of the system. Also, the maximum entropy generation takes place at the interface between clear fluid and fluid saturated porous medium.

2. Problem definition

The schematic diagram of the problem is shown in Fig. 1. Laminar fluid flow with constant thermophyiscal properties in a conduit partially filled with porous medium is considered. Fluid stream with a uniform velocity and temperature is considered at the inlet to the conduit. The wall temperature of the conduit is fixed, and assumed that it is higher than the inlet temperature.

2.1. Governing equations

The flow is assumed to be two-dimensional and steady. It is also assumed that buoyancy effects are negligible. The governing equations may be written as:

continuity

$$\frac{\partial}{\partial z}(\rho u)+\frac{1}{r^n}\frac{\partial}{\partial r}(r^n\rho v)=0 \tag{2}$$

z-momentum

$$\begin{aligned}\frac{\partial}{\partial z}(\rho uu)+\frac{1}{r^n}\frac{\partial}{\partial r}(r^n\rho vu)&=-\frac{\partial p}{\partial z}+\frac{\partial}{\partial z}\left(\mu_e\frac{\partial u}{\partial z}\right)+\frac{1}{r^n}\frac{\partial}{\partial r}\left(r^n\mu_e\frac{\partial u}{\partial r}\right)\\&\quad-f\frac{\mu_e u}{K}-f\frac{\rho F}{\sqrt{K}}|u|u\end{aligned} \tag{3}$$

r-momentum

$$\begin{aligned}\frac{\partial}{\partial z}(\rho uv)+\frac{1}{r^n}\frac{\partial}{\partial r}(r^n\rho vv)&=-\frac{\partial p}{\partial r}+\frac{\partial}{\partial z}\left(\mu_e\frac{\partial v}{\partial z}\right)+\frac{1}{r^n}\frac{\partial}{\partial r}\left(r^n\mu_e\frac{\partial v}{\partial r}\right)\\&\quad-f\frac{\mu_e v}{K}-f\frac{\rho F}{\sqrt{K}}|u|v-\frac{\mu_e v}{r^2}n\end{aligned} \tag{4}$$

For flow in a pipe (axi-symmetric) n is set to unity and for flow in channel, n is set to zero. The parameter f is set to unity for flow in porous medium and to zero for flow in a region without porous material. Note that flux continuity (momentum and energy) is ensured by evaluating the harmonic mean values of the physical properties (viscosity, thermal conductivity) at the interface between the clear fluid and the fluid-saturated porous medium.

Fig. 1. Schematic diagram of the problem.

2.2. Energy equation

The energy equation, while neglecting viscous dissipation effect and heat generation, may be written as:

$$\frac{\partial}{\partial}(\rho_e c_e u T) + \frac{1}{r^n}\frac{\partial}{\partial r}(\rho_e c_e r^n v T) = \frac{\partial}{\partial z}\left(k_e \frac{\partial T}{\partial z}\right) + \frac{1}{r^n}\frac{\partial}{\partial r}\left(r^n k_e \frac{\partial T}{\partial r}\right) \quad (5)$$

where k_e, c_e and ρ_e are the effective thermal conductivity, effective specific heat and effective density of the medium, respectively.

In modeling of the energy transport, it is assumed that the local thermal equilibrium exists between solid and fluid phases. Thermal equilibrium condition is adopted by Kaviany [11]. Also, previous work of Mohamad and Karim [20] revealed that the thermal equilibrium assumption is valid as far as there is no heat released in the fluid phase (combustion for instance) or in solid phase (catalytic effect for instance). Moreover, a few tests done with two energy equation and it is found that the results are not that sensitive to the non-equilibrium condition. Therefore, it is assumed that thermal equilibrium is valid.

Axi-symmetric boundary conditions are adopted at $r = 0$, i.e., $v = 0$ with the gradients of u and T in the r-direction set to zero. The v velocity component is set to zero, $u = u_{in}$ and $T = T_{in}$ at $z = 0$. For $z = L$, the gradients of the variables in the z-direction are set to zero. For $r = r_o$ and $0 < z < L$, no slip condition is assumed, i.e., $u = v = 0$ and $T = T_w$.

The above equations are non-dimensionalized by using the inlet velocity, inlet temperature, and the conduit (radius or half height) as references to scale velocity components, temperature and length, respectively. Hence, the momentum and energy equations may be reformulated as:

Z-momentum

$$\frac{\partial}{\partial Z}(UU) + \frac{1}{R^n}\frac{\partial}{\partial R}(R^n VU) = -\frac{\partial P}{\partial Z} + \frac{1}{Re}\left[\frac{\partial}{\partial Z}\left(\frac{\partial U}{\partial Z}\right) + \frac{1}{R^n}\frac{\partial}{\partial R}\left(R^n \frac{\partial U}{\partial R}\right)\right] - f\frac{U}{Da\,Re} \quad (6)$$

R-momentum

$$\frac{\partial}{\partial Z}(UV) + \frac{1}{R^n}\frac{\partial}{\partial R}(R^n VU) = -\frac{\partial P}{\partial R} + \frac{1}{Re}\left[\frac{\partial}{\partial Z}\left(\frac{\partial V}{\partial Z}\right) + \frac{1}{R^n}\frac{\partial}{\partial R}\left(R^n \frac{\partial V}{\partial R}\right)\right] - f\frac{V}{Da\,Re} - f\frac{V}{Re\,R^2}n \quad (7)$$

energy equation

$$\frac{\partial}{\partial Z}(U\theta) + \frac{1}{R^n}\frac{\partial}{\partial R}(R^n V\theta) = \frac{1}{Pe}\left(\frac{\partial^2\theta}{\partial Z^2}\right) + \frac{1}{Pe\,R^n}\frac{\partial}{\partial R}\left(R^n\frac{\partial\theta}{\partial R}\right) \quad (8)$$

2.3. Entropy generation calculations

The volumetric rate of entropy generation arises due to the heat transfer and friction losses. For a conduit partially filled with porous media, the entropy generation can be written as Bejan [1],

$$e_g = \frac{k}{T_o^2}[\nabla T^2] + (1-f)\frac{\mu\Phi}{T_o} + f\frac{\mu}{KT_o}[\vec{v}]^2. \quad (9)$$

The first term is the rate of entropy generation due to heat transfer and the last two terms are due to friction. For region porous media the last term become important compared with second term. As a usual practice, the last term is set to zero for region without porous medium and second term set to zero for region with porous medium. The heat dissipation term due to friction (Φ) for axi-symmetric flow conditions can be expressed as Bird et al. [21],

$$\Phi = 2\left[\left(\frac{\partial v}{\partial r}\right)^2 + \left(\frac{v}{r}n\right)^2 + \left(\frac{\partial u}{\partial z}\right)^2\right] + \left[\frac{\partial v}{\partial z} + \frac{\partial u}{\partial r}\right]^2 \quad (10)$$

The dimensionless form for entropy generation can written in final form substituting Eq. (10) into Eq. (9),

$$E_g = \left(\frac{\partial\theta}{\partial Z}\right)^2 + \left(\frac{\partial\theta}{\partial R}\right)^2 + (1-f)Br_m\left\{2\left[\left(\frac{\partial V}{\partial R}\right)^2 + \left(\frac{V}{R}n\right)^2 + \left(\frac{\partial U}{\partial Z}\right)^2\right] + \left[\frac{\partial V}{\partial Z} + \frac{\partial U}{\partial R}\right]^2\right\} + f\frac{Br_m}{Da}[\vec{V}]^2 \quad (11)$$

The parameter that controls entropy generation for fluid flow without porous material is modified Brinkman number and for flow in a porous media the controlling parameter is ratio of modified Brinkman to Darcy number. For a fixed modified Brinkman number, decreasing Darcy number, less permeable media, enhances entropy generation due to high pressure drop and friction losses.

2.4. Nusselt number calculations

The Nusselt number for a pipe can be calculated as:

$$Nu_D = \frac{2\frac{\partial\theta}{\partial R}}{\theta_w - \theta_m} \quad (12)$$

The bulk temperature for flow in a pipe and in a channel can be calculated as:

$$\theta_m = \frac{\int_0^1 U\theta R^n \, dR}{\int_0^1 UR^n \, dR} \tag{13}$$

3. Method of solution

3.1. Numerical solution

A control volume, finite-difference approach is used to solve the model equations with specified boundary conditions. The SIMPLER algorithm is employed to solve the equations in primitive variables. Central difference approximations are used to approximate the advection–diffusion terms, i.e., the scheme is second order accurate in space. The governing equations are converted into a system of algebraic equations through integration over each control volume. The algebraic equations are solved by a line-by-line iterative method. The method sweeps the domain of integration along the R and Z-axis and uses the tri-diagonal matrix inversion algorithm to solve the system of equations. Velocity components are under-relaxed by a factor of 0.7. For most calculations, 4000 iterations are sufficient to get convergent solution for a 151×81 grid, and more iteration is needed for 201×101. The criteria for convergence are to conserve mass, momentum, energy and species globally and locally, and to ensure convergence of preselected dependent variables to constant values within machine error.

In order to insure that the results are grid size independent, different meshes are tested namely 121×61, 151×81 and 201×101. The predicted results are compared for flow in a pipe without porous media. The

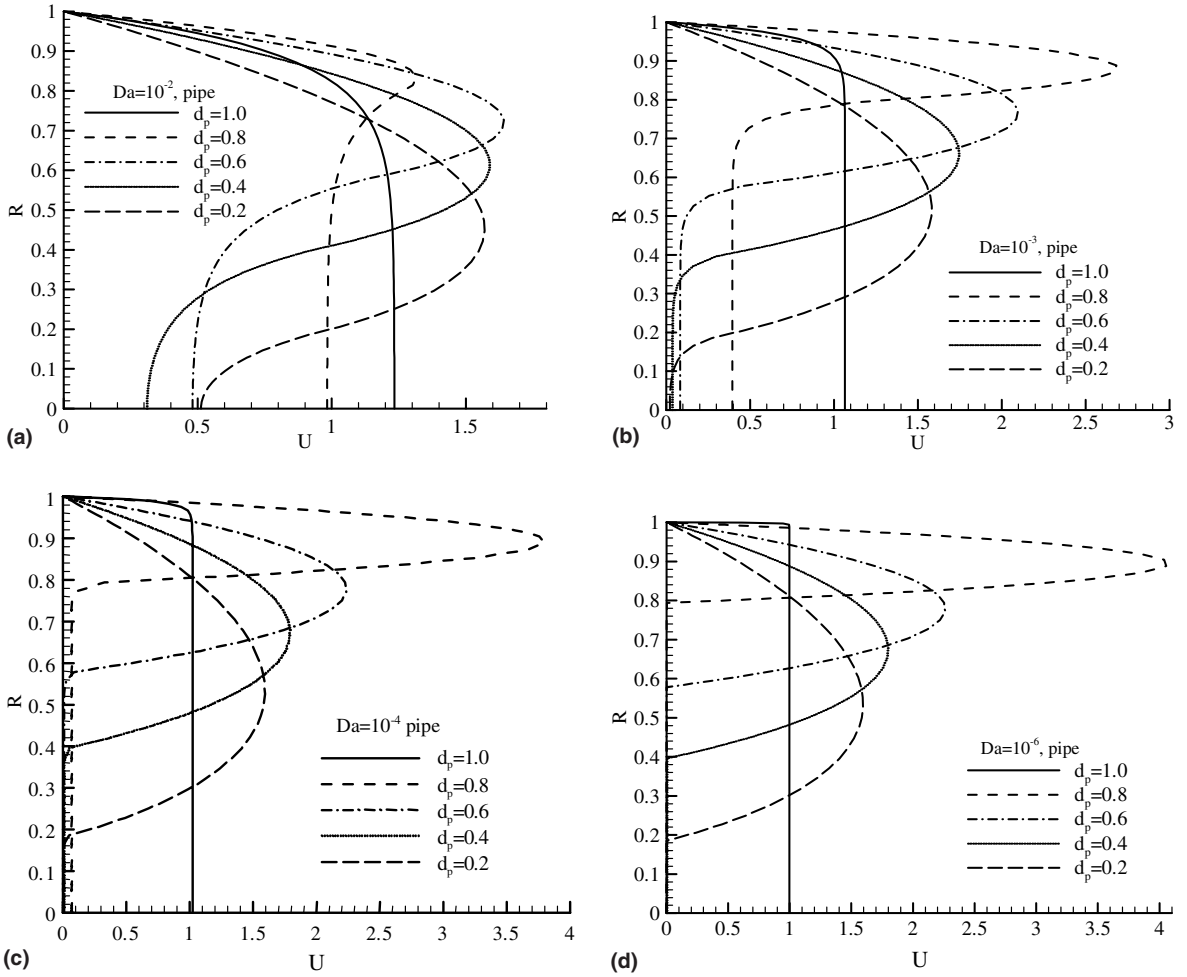

Fig. 2. Fully developed velocity profiles in a pipe partially filled with porous medium and for (a) $Da = 10^{-2}$; (b) $Da = 10^{-3}$; (c) $Da = 10^{-4}$; (d) $Da = 10^{-6}$.

developed velocity profile (parabolic) is compared with analytical solution and difference was not noticeable. The test was done for different Reynolds numbers and found that the developing length is inversely proportional of Reynolds number, which matches the analytical solution. Furthermore, the local Nusselt numbers along the pipe and the channel were well compared with analytical solutions. Since, results are available for a pipe and a channel fully filled with porous media, the predicted results were well compared with Nusselt number and velocity profile was uniform, except near the boundary. Quantative comparison of the current results with available data will be presented in the following section. The calculations are performed by adopting non-uniform 151×61 grids in z- and r-direction, respectively. Very fine grids are adopted near the boundaries. All the calculations were performed using double precision, which is necessary for the Nusselt number calculations.

3.2. Analytical solution

It is possible to obtain an analytical solution for fully developed condition. The dimensionless z-momentum equation for flow in a region without porous material can be written for the fully developed condition as:

$$0 = -\frac{dP}{dZ} + \frac{1}{Re}\left[\frac{1}{R^n}\frac{d}{dR}\left(R^n\frac{dU}{dR}\right)\right] \tag{14a}$$

The momentum equation for flow in saturated porous material can be written as:

$$0 = -\frac{dP}{dZ} - \frac{U}{Da\,Re} \tag{14b}$$

Eq. (14b) is valid for R from zero (center of the pipe) to radius equal to R_p, while Eq. (14a) is valid from $R = R_p$ to $R = 1$. Assuming the velocity continuity at the interface between the fluid and fluid saturated

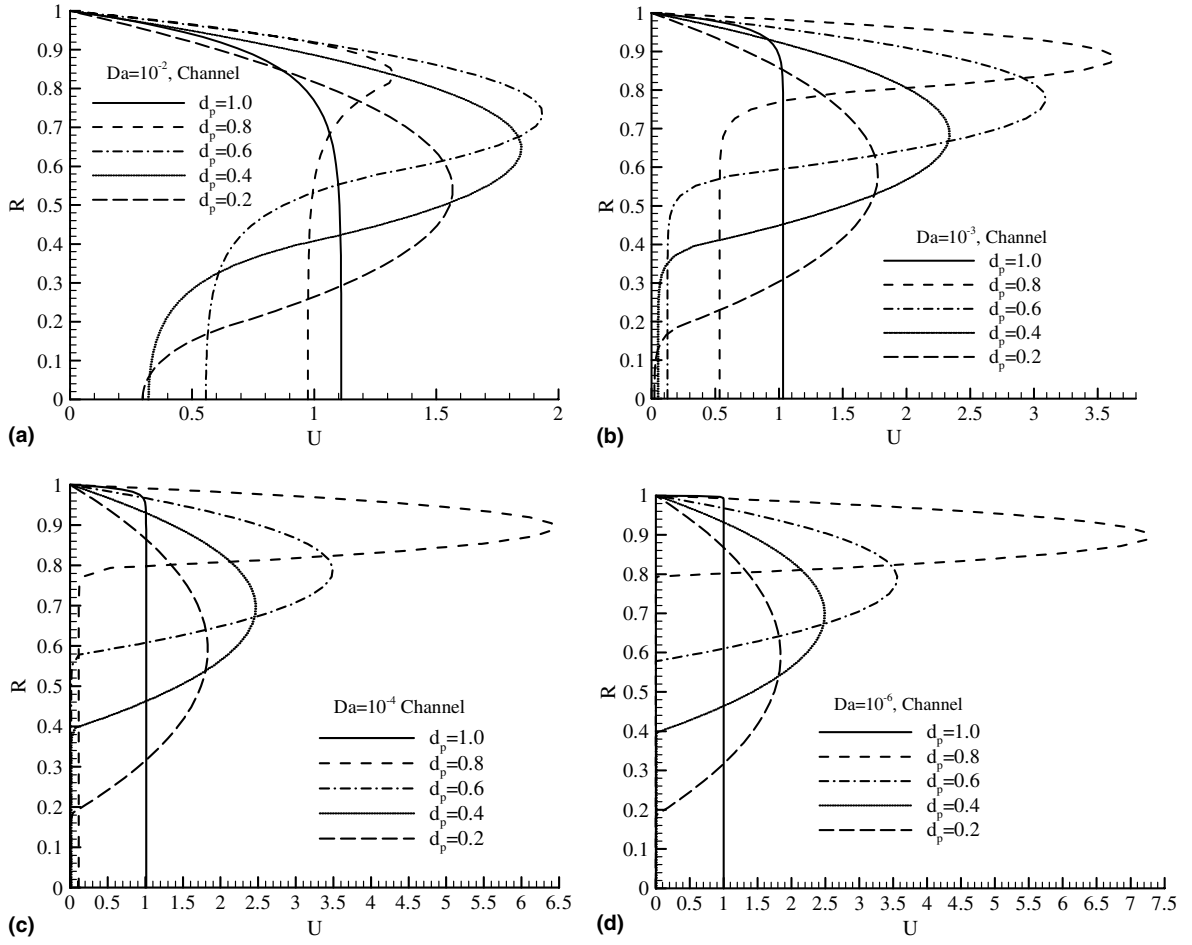

Fig. 3. Fully developed velocity profiles in a channel partially filled with porous medium and for (a) $Da = 10^{-2}$; (b) $Da = 10^{-3}$; (c) $Da = 10^{-4}$; (d) $Da = 10^{-6}$.

porous medium, it is possible to solve the Eq. (14a) and (14b) and velocity profile for circular tube can be written as:

$$U = -\frac{8Da\ln(R_p)}{(R_p^2-1)\left[1-4Da-R_p^2+(1+R_p^2)\ln(R_p)\right]}$$

for $0 \leqslant R \leqslant R_p$ (15a)

and

$$U = -\frac{2\left[(4Da-1+R_p^2)\ln(R)-(R^2-1)\ln(R_p)\right]}{(R_p^2-1)\left[1-4Da-R_p^2+(1+R_p^2)\ln(R_p)\right]}$$

for $R_p \leqslant R \leqslant 1$ (15b)

The flow velocity is constant in the saturated porous region.

For flow in ducts the velocity profile can be written as

for $0 \leqslant Y \leqslant Y_p$

$$U = \frac{12Da}{6Da(1+Y_p)-(Yp-1)^3} \quad (16a)$$

and

for $Y_p \leqslant Y \leqslant 1$

$$U = -\frac{6(Y-1)\left[2Da-(Y-Y_p)(Y_p-1)\right]}{(Y_p-1)\left[(Y_p-1)^3-6Da(Y_P+1)\right]} \quad (16b)$$

Also, the entropy generation for flow in a region with out porous material and fully developed conditions can be simplifies as:

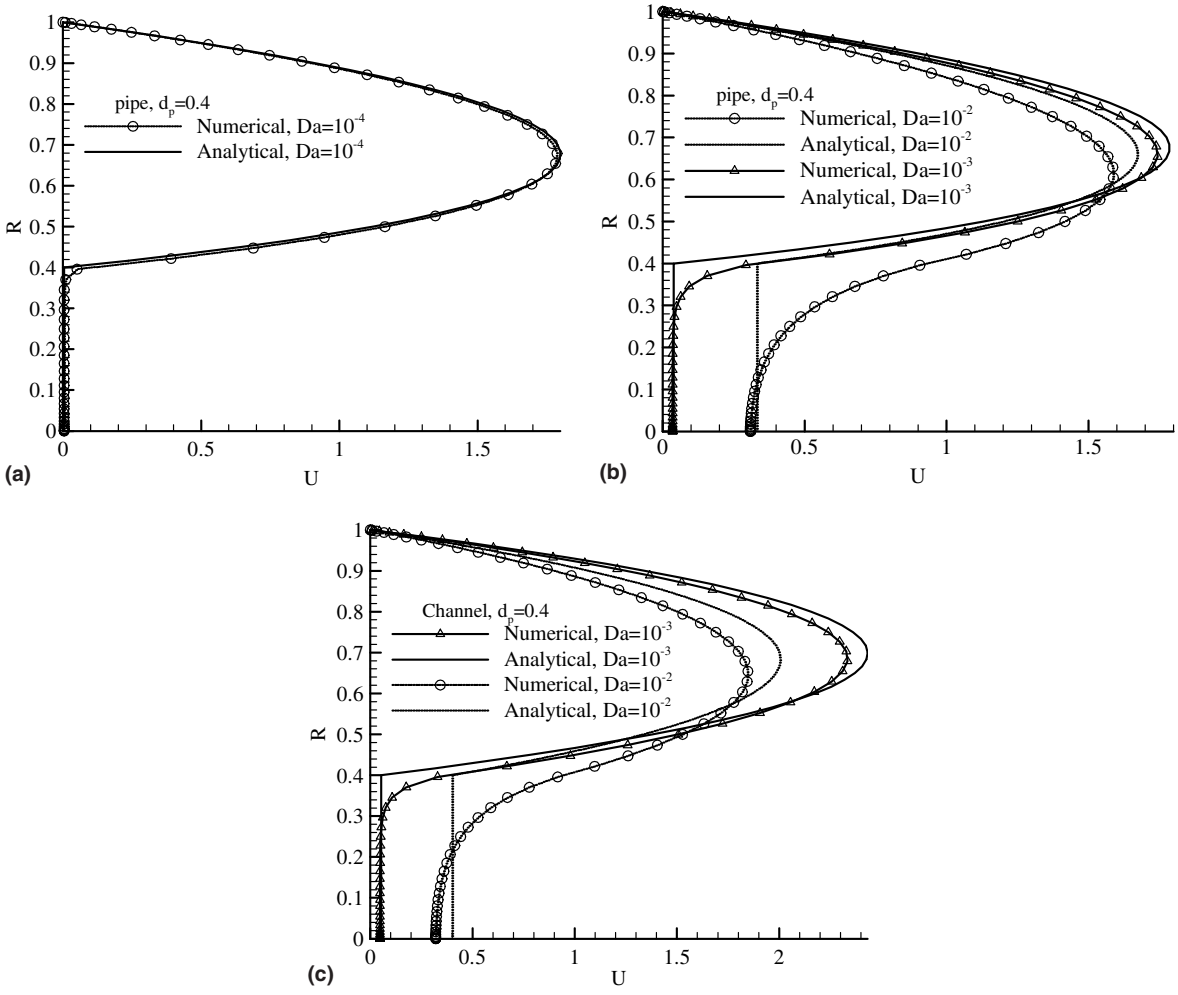

Fig. 4. Comparison of velocity profile obtain numerically and analytically for flow in a pipe for (a) $d_p = 0.4$ and $Da = 10^{-4}$; (b) $d_p = 0.4$, for $Da = 10^{-2}$ and $Da = 10^{-3}$; (c) $d_p = 0.4$, for $Da = 10^{-2}$ and $Da = 10^{-3}$.

$$E_g = \left(\frac{\partial\theta}{\partial Z}\right)^2 + \left(\frac{\partial\theta}{\partial R}\right)^2 + Br_m\left\{\left[\frac{\partial U}{\partial R}\right]^2\right\} \quad (17)$$

The entropy generation for the region with saturated porous material can be written as:

$$E_g = \left(\frac{\partial\theta}{\partial Z}\right)^2 + \left(\frac{\partial\theta}{\partial R}\right)^2 + \frac{Br_m}{Da}[U]^2 \quad (18)$$

From numerical analysis (which will be discussed later on), the thermal contribution for entropy generation is not that significant compared with that of mechanical. Hence, if the thermal contribution to the entropy generation is neglected the entropy generation for the fully developed condition can be written as:

Tube

for $0 \leqslant R \leqslant R_p$

$$E_g = Br_m Da\left[\frac{8\ln(R_p)}{(R_p^2-1)\left[1-4Da-R_p^2+(R_p^2+1)\ln(R_p)\right]}\right]^2 \quad (19a)$$

and

for $R_p \leqslant R \leqslant 1$

$$E_g = Br_m\left[\frac{2(4Da-1+R_p^2)\frac{1}{R}-2R\ln(R_p)}{(R_p^2-1)\left[1-4Da-R_p^2+(R_p^2+1)\ln(R_p)\right]}\right]^2 \quad (19b)$$

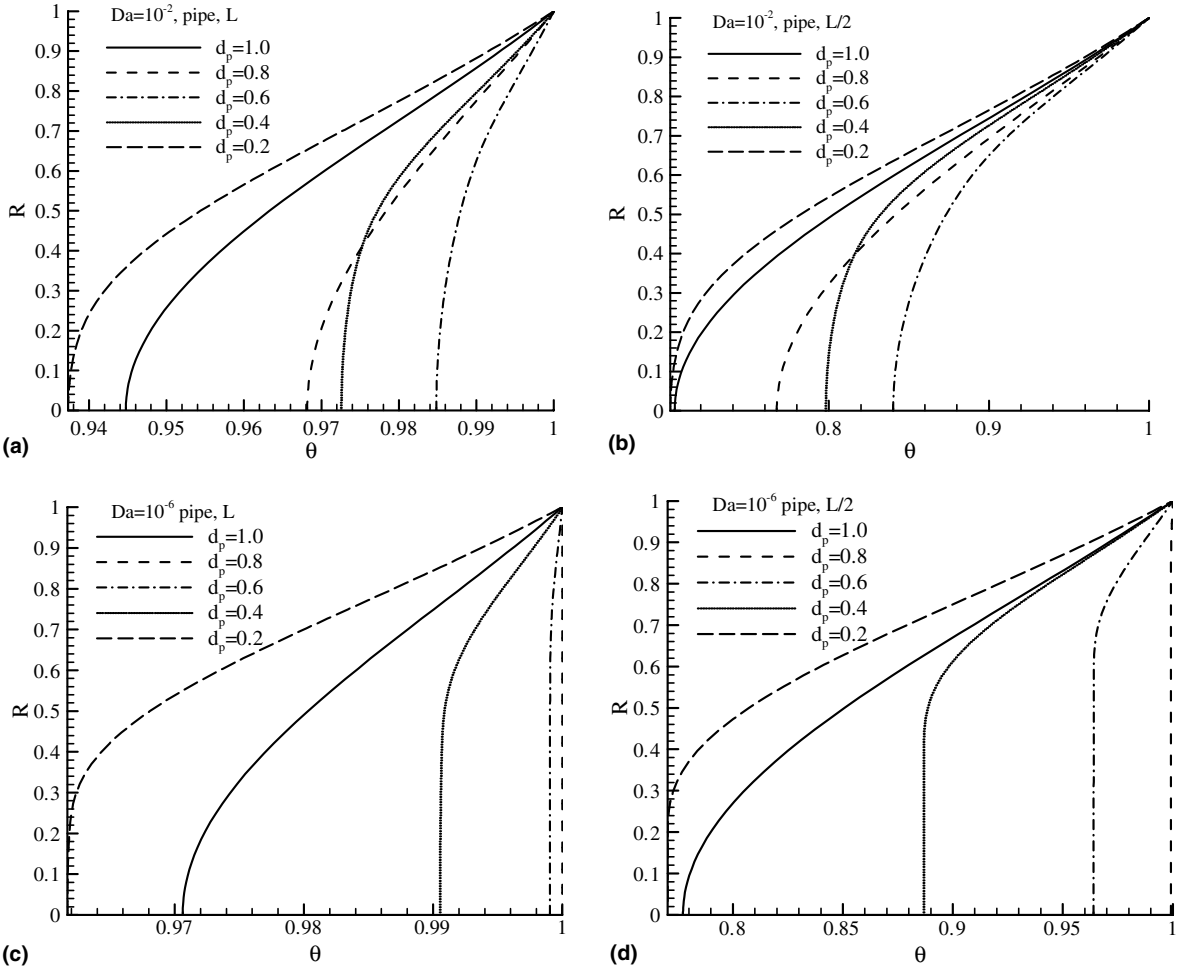

Fig. 5. Temperature profile for different porous layer radius and for (a) $Da = 10^{-2}$, at the exit of the pipe; (b) $Da = 10^{-2}$, at the middle length of the pipe; (c) $Da = 10^{-6}$, at the exit of the pipe; (d) $Da = 10^{-6}$, at the middle length of the pipe.

Duct

for $0 \leqslant Y \leqslant Y_p$

$$E_g = Br_m Da \left[\frac{12}{6Da(Y_p + 1) - (Y_p - 1)^3} \right]^2 \quad (20a)$$

and

for $Y_p \leqslant Y \leqslant 1$

$$E_g = Br_m \left[\frac{6(Y-1)\left[2Da - (Y - Y_P)(Y_p - 1)\right]}{(Y_p - 1)\left[(Y_p - 1)^3 - 6Da(Y_p + 1)\right]} \right]^2 \quad (20b)$$

4. Results and discussion

It is know that the fully developed flow in a tube and rectangular duct without porous have a parabolic velocity profiles with non-dimensional center velocity of 2.0 and 1.5, respectively. The numerical solution predicted the velocity profiles for both cases within machine error. Also, the Nusselt number for constant wall temperature is 3.66 and 7.54, for tube and channel, respectively. The predicted results were consistent with the analytical results. For details we referee to Mohamad [7]. The objective of this work is to analyze the entropy generation associated with flow in tube and channel fully or partially filled with porous medium.

The mechanism of entropy generation in a system can be classed as thermal and mechanical. Whenever, there is a heat transfer, i.e., temperature gradient in the system and/or between the system and surrounding, entropy generates (thermal), which depends on the temperature gradient (Eq. (11), first two terms). Furthermore, the entropy generates due to internal and external friction (mechanical) in a conduit without porous

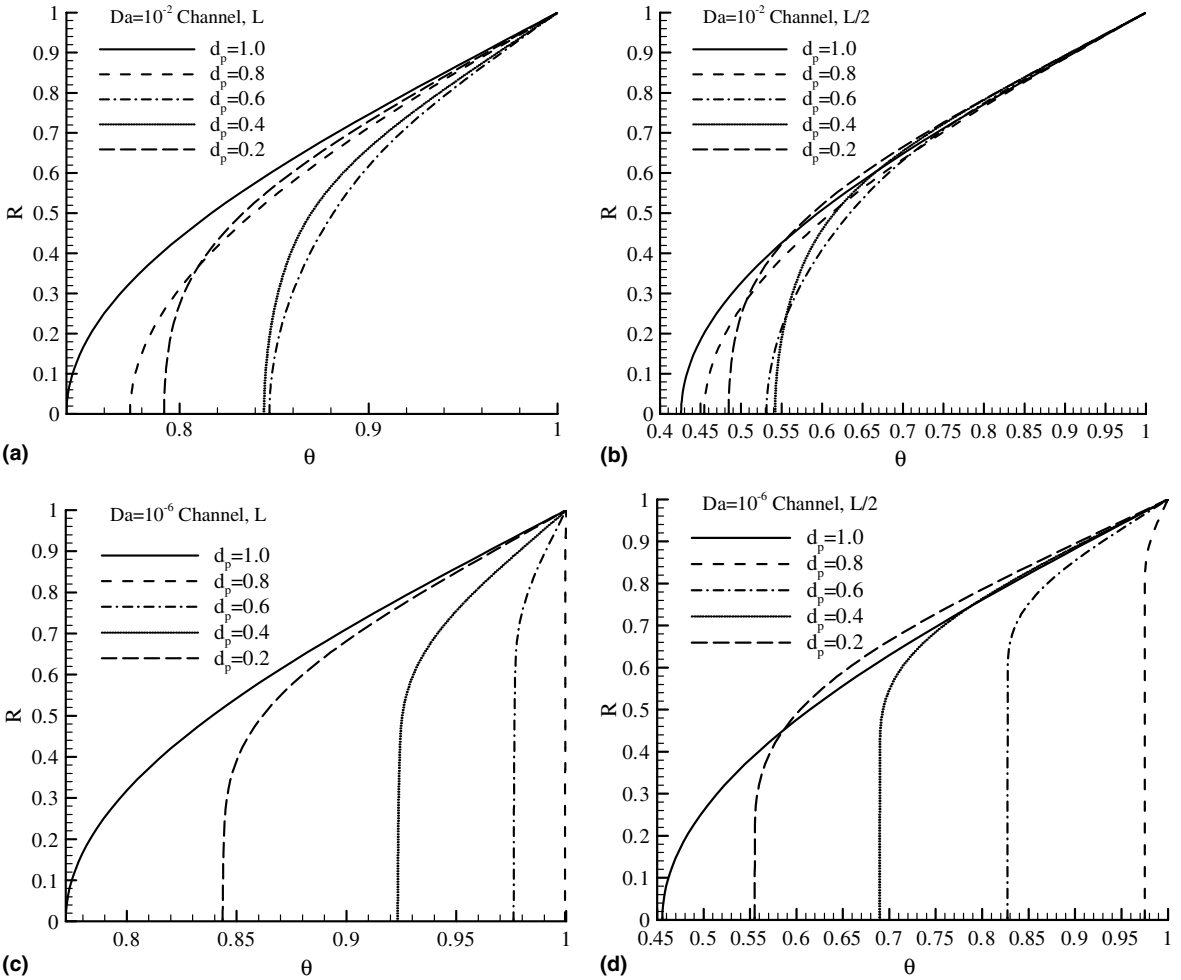

Fig. 6. Temperature profile for different porous layer radius and for (a) $Da = 10^{-2}$, at the exit of the channel; (b) $Da = 10^{-2}$, at the middle length of the channel; (c) $Da = 10^{-6}$, at the exit of the channel; (d) $Da = 10^{-6}$, at the middle length of the channel.

medium, which depends on the velocity gradient, i.e., shear stress (Eq. (11), third term). Porous medium adds extra flow resistance, drag and friction between the flow and solid surfaces, consequently entropy generates, which mainly depends on the velocity of the flow in the medium and permeability of the medium (Darcy number) as it is represented in the last term of the Eq. (11). Hence, it is essential to understand the temperature and velocity field of the flow in order to fully gauge the entropy generation in the system.

Figs. 2 and 3 show the fully developed velocity profiles for different Darcy parameter and porous thickness and for flow in tube and channel, respectively. It is clear that the Darcy model is not valid for $Da > 10^{-4}$ (high porous medium), where the viscous and inertia terms become important in the porous region. The velocity is not constant in the porous layer. If the porous material is not fully occupy the conduit, the flow almost diminishes as the Da decreases less than 10^{-4} in the porous region. The analytical solution predicts velocity profile accurately for $Da = 10^{-4}$ as shown in Fig. 4a. The analytical solution is fairly in agreement with the numerical solution for $Da > 10^{-4}$, Fig. 4b and c. Since, the analytical solution is based on Darcy model for flow in porous media, the interface region is not in good agreement between analytical and numerical solution. In fact, it is possible to get better agreement between analytical solution and numerical solution, if the diffusion term is retained in the porous medium region for $Da > 10^{-4}$. The velocity profiles presented before help us in explaining the trend of entropy generation in the fully developed region due to friction and drag forces.

To understand the thermal entropy generation, a need arises to inspect temperature field. Figs. 5 and 6 show temperature profiles as function of porous layer thickness for tube, and channel flows, respectively, for $Da = 10^{-2}$ and $Da = 10^{-6}$ and for two position at the outlet and half length of the conduit. The general trend

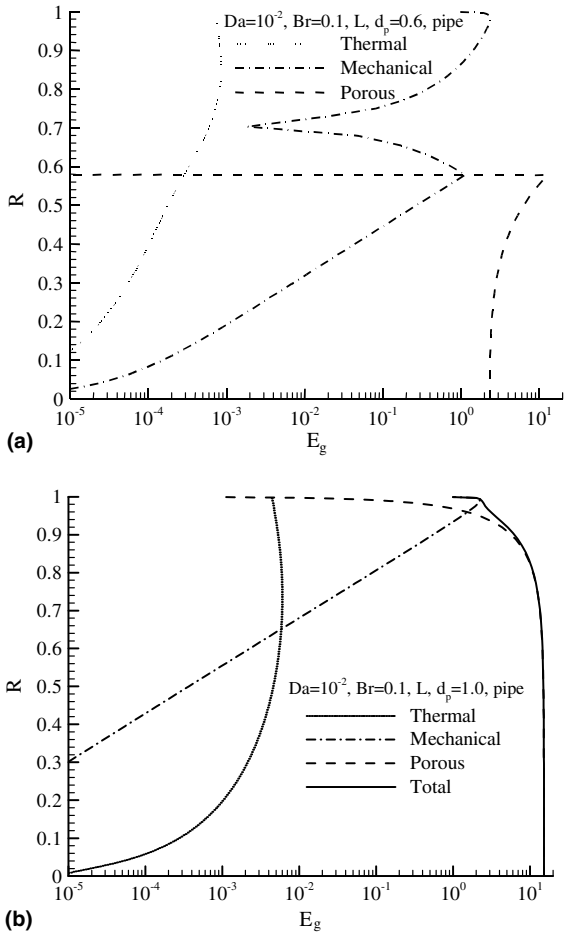

Fig. 7. Profile of entropy generation for (a) $Da = 10^{-2}$, $d_p = 0.6$ at the exit of the pipe; (b) $Da = 10^{-2}$ for the pipe fully filled with porous medium.

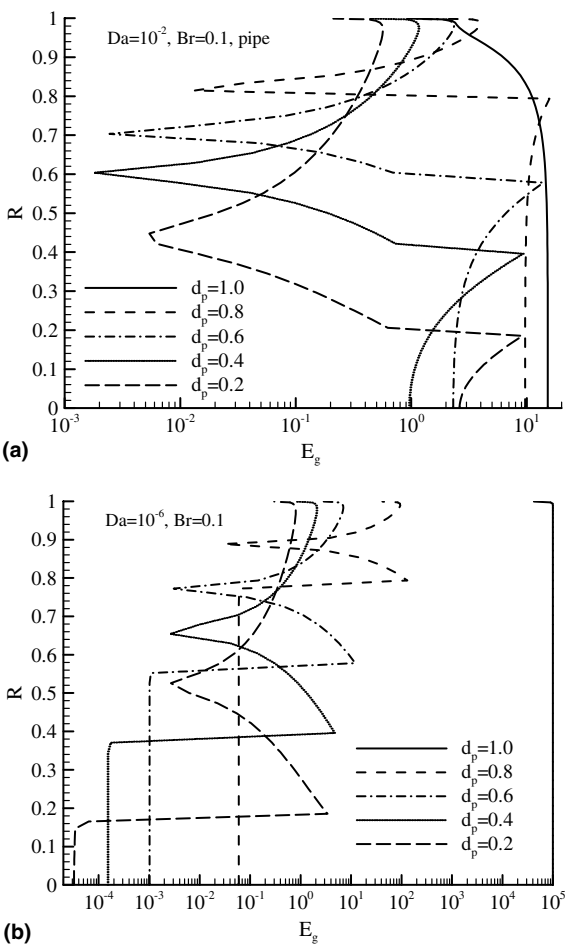

Fig. 8. Total entropy generation for (a) $Da = 10^{-2}$; (b) $Da = 10^{-6}$ and for different porous layer thickness.

is that for $d_p = 0.6$ the temperature is almost uniform across the cross section at the outlet of the conduit. The temperature gradient is almost zero at the core region of the conduit, except for full filled conduit with porous medium. For the region near the solid boundary the temperature gradient depends on the porous layer. In general as the porous layer thickness decreases the temperature gradient increases, except for fully filled conduit. The mentioned trend is valid for temperature profile at the outlet of the conduit.

The following paragraphs discuss the entropy budget analysis and entropy development along the conduit for different Darcy parameters and porous layer thickness.

The entropy generation budget analysis is shown in Fig. 7 for $Da = 10^{-2}$, $Br = 0.1$ and for d_p of 0.6 and 1.0, respectively. The dominant mechanism of entropy generation is due to viscous and drags force between flow and porous solid surface. The entropy generation due to heat transfer can be neglected without introducing noticeable error. However, the results presented for $Br_m = 0.1$, it is expected that the thermal entropy generation compared with that of the friction become important as Br_m decrease, i.e., rate of heating or cooling increases (ΔT increases).

For tube partially filled with porous media, the entropy generation in the porous region is the dominated by the friction and drag forces between flow and porous solids. The second contribution comes from shear stress if Darcy number is greater than $Da = 10^{-4}$. For region without porous medium, the mechanical entropy generation is higher at the interface region and at the wall due to shear stress, Fig. 7a. The entropy generation decreases between the mentioned boundaries and reaches minimum value at the point where the velocity profile reaches the maximum value (Fig. 2a). These results are

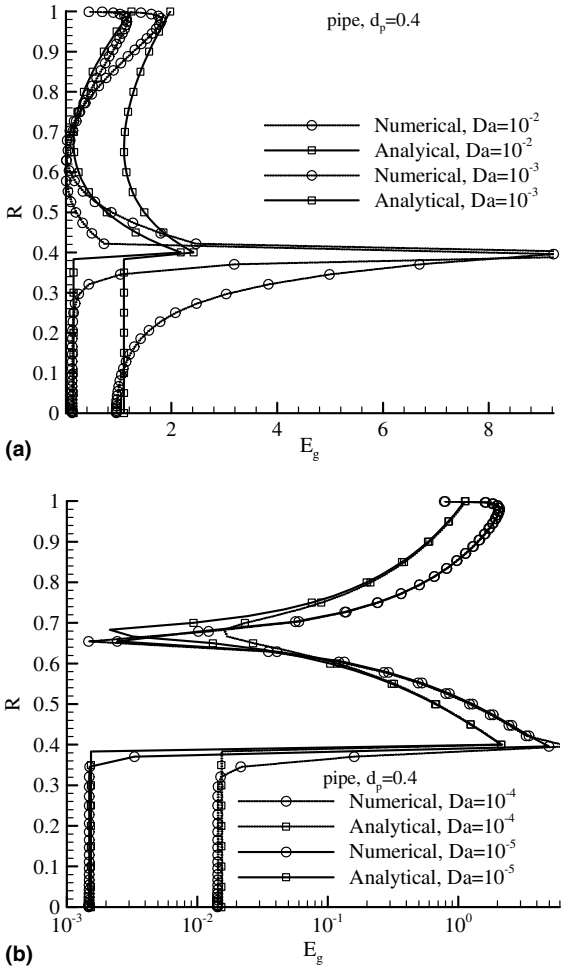

Fig. 9. Comparison between numerical and analytical solutions in predicting total entropy generation in a pipe filled with porous medium partially and for (a) $Da = 10^{-2}$ and $Da = 10^{-3}$; (b) $Da = 10^{-4}$ and $Da = 10^{-5}$.

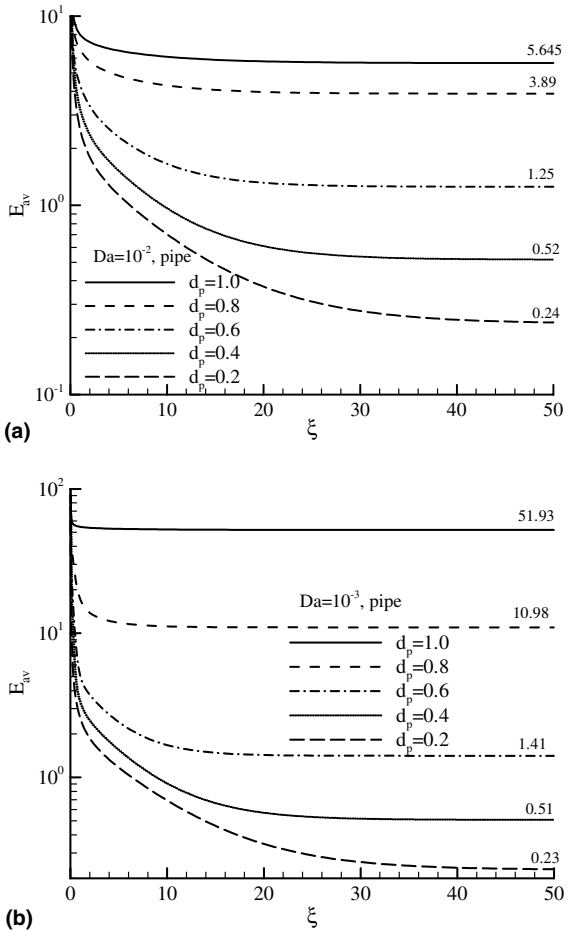

Fig. 10. Cross sectional average of the total entropy generation variation along the pipe for (a) $Da = 10^{-2}$; (b) $Da = 10^{-3}$ and for different d_p.

typical for other Darcy numbers and conduit shapes. Hence, there is no need to show more figures.

Fig. 8a and b show the total entropy generation for $Da = 10^{-2}$ and $Da = 10^{-6}$, respectively. The trend is as follow, the entropy generation has highest value at the interface between the flows saturated porous medium and clear flow. The entropy generation reaches the minimum value at the region where the velocity reaches the highest value with zero gradients. The total entropy generation increases as the porous layer thickness increases and reaches highest value for conduit fully filled with porous medium.

Analytical solution predicts the entropy generation quite well for $Da \leqslant 10^{-4}$ as shown in Fig. 9, but the analytical solution fails to produce correct results at the interface for $Da > 10^{-4}$ as shown in Fig. 9a, because the analytical solution based on Darcy model.

The cross sectional average total entropy generations along the conduit are shown in Figs. 10 and 11 for tube and channel flows, respectively. Entropy generation asymptotically decreases to a constant value as the fully developed condition reaches. As the Darcy number decreases and/or porous layer thickness increases, the entropy generation increases.

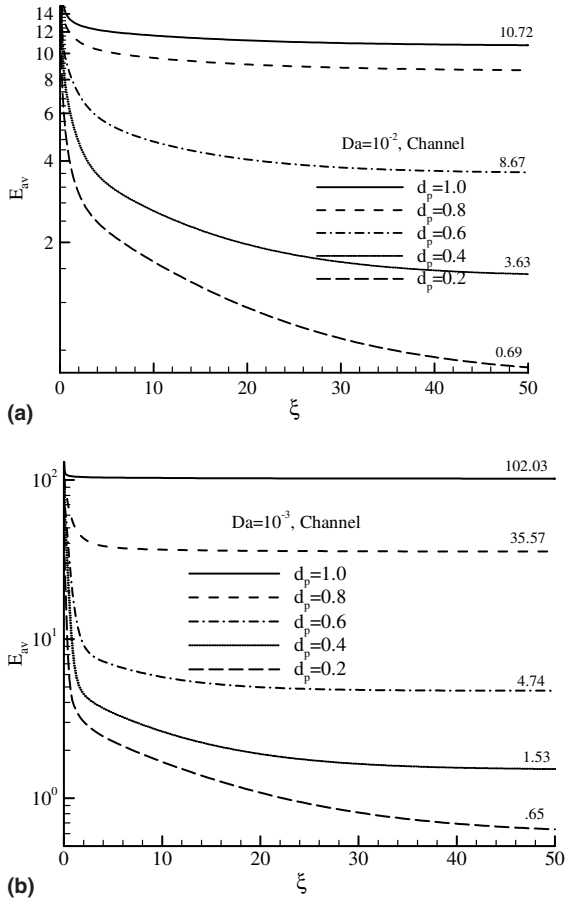

Fig. 11. Cross sectional average of the total entropy generation variation along the channel for (a) $Da = 10^{-2}$; (b) $Da = 10^{-3}$ and for different d_p.

5. Conclusions

Numerical and analytical solutions are performed to investigate the entropy generation in flows through heated, isothermal pipes and ducts. The analytical solution is based on Darcy law for the flow in porous region. The analytical solution is accurate for Darcy parameter greater that about 10^{-4}. The mechanism of entropy generation in the conduit is mainly dominated by friction and drag force in the porous medium. The maximum entropy generation occurs at the interface between the flow in porous medium and clear flow. The entropy generation showed minimum value in the region where the velocity shows the peak value, i.e., zero gradients. The total entropy generation increases as the Darcy parameter decrease and/or porous layer increase and reaches maximum value for flow in a conduit fully filled with porous medium. Also, the entropy generation has highest value at the entrance region and asymptotically deceases to a constant value as the flow reaches fully developed condition.

Acknowledgment

The author gratefully acknowledge the support of the DAAD—German Academic Exchange Service (Kennziffer A/03/0482, Haushaltstitel 331 4 03 151) for work in Institute for Energy Engineering at Technical University of Berlin and Professor A.A. Mohamad (Department of Mechanical and Manufacturing Engineering, The University of Calgary) for the possibility of using computer programs for numerical data.

References

[1] A. Bejan, Entropy Generation through Heat and Fluid Flow, John Wiley and Sons, New York, 1982.
[2] A. Bejan, G. Tsatsaronis, M. Moran, Thermal Design and Optimization, John Wiley and Sons, New York, 1996.
[3] A. Bejan, Entropy generation minimization in heat transfer. In: E. Sciubba, M. Moran (Eds.) Second Law Analysis of Energy systems: toward the 21st century. Proceedings of International Conferences ROMA', 1995, pp. 363–372.
[4] S. De Olivera, B. Schwarzer, P. Le Goff, D. Tondeur. Comparison of the entropic, exergetic and economic optima of a heat exchanger, in: D. Kouremenos, G. Tsatsaronis, C. Rakopoulos (Eds.) Proceedings of International Conference ATHENS'91 Analysis of Thermal and Energy Systems, 1991, pp. 105–116.

[5] L. Robert, M. Feidt, Optimisation dynamique du comportement d'un echanger de chaleur soumis au phenomene d'encrassement, Entropie 226 (2000) 28–36.
[6] T. Morosuk, Porous media theory for fouling problems in heat exchangers of refrigeration machines and heat pumps, on current issues on heat and mass transfer in porous media, in: Proceedings of the NATO Advanced Study Institute on Porous Media, 9–20 June 2003, Neptun, Romania, 2003, pp. 406–416.
[7] A.A. Mohamad, Heat transfer enhancements in heat exchangers fitted with porous media Part I: constant wall temperature, Int. J. Therm. Sci. 42 (2003) 385–395.
[8] R.L. Webb, Principles of Enhanced Heat Transfer, Wiley, New York, 1994.
[9] G. Lauriat, R. Ghafir, Forced convective transfer in porous media, in: K. Vafai, H.A. Hadim (Eds.), Handbook of Porous Media, Marcel Dekker, New York, 2000.
[10] A.A. Mohamad, High Efficiency Solar Air Heater, Solar Energy 60 (1997) 71–76.
[11] M. Kaviany, Laminar flow through a porous channel bounded by isothermal parallel plates, Int. J. Heat Mass Transfer 28 (1985) 851–858.
[12] D. Poulikakos, M. Kazmierczak, Forced convection in a duct partially filled with a porous material, ASME J. Heat Transfer 109 (1987) 653–662.
[13] J.Y. Jang, J.L. Chen, Forced convection in a parallel plate channel partially filled with a high porosity medium, Int. Commun. Heat Mass Transfer 19 (1992) 263–273.
[14] S. Chikh, A. Boumedien, K. Bouhadef, G. Lauriat, Analytical solution of non-Darcian forced convection in an annular duct partially filled with a porous medium, Int. J. Heat Mass Transfer 38 (1995) 1543–1551.
[15] S. Chikh, A. Boumedien, K. Bouhadef, G. Lauriat, Non-Darcian forced convection analysis in an annular duct partially filled with a porous medium, Numer. Heat Transfer 28 (1995) 707–722.
[16] M.A. Al-Nimr, M.K. Alkam, Unsteady Non-Darcian forced convection analysis in an annulus partially filled with a porous material, ASME J. Heat Transfer 119 (1994) 799–804.
[17] M.K. Alkam, M.A. Al-Nimr, M.O. Hamdan, Enhancing heat transfer in parallel-plate channels by using porous inserts, Int. J. Heat Mass Transfer 44 (2001) 931–938.
[18] B.A. Abu-Hijleh, M.A. Al-Nimr, The effect of the local inertial term on the fluid flow in channels partially filled with porous material, Int. J. Heat Mass Transfer 44 (2001) 1565–1572.
[19] J.L. Lage, A. Narasimhan, Porous media enhanced forced convection fundamentals and applications, in: K. Vafai, H.A. Hadim (Eds.), Handbook of Porous Media, Marcel Dekker, New York, 2000.
[20] A.A. Mohamad, G.A. Karim, Flow and heat transfer within segregated beds of solid particles, J. Porous Media 4 (3) (2001) 215–224.
[21] R.B. Bird, W.E. Stewart, E.N. Lightfoot, Transport Phenomena, second ed., John Wiley and Sons, New York, 2001.